

# Amphiphilic Perylenetetracarboxyl Diimide Dimer and Its Application in Field Effect Transistor

Yanfeng Wang,<sup>†</sup> Yanli Chen,<sup>†,‡</sup> Renjie Li,<sup>†</sup> Shuangqing Wang,<sup>§</sup> Wei Su,<sup>†</sup> Pan Ma,<sup>†</sup>  
Michael R. Wasielewski,<sup>||</sup> Xiyou Li,<sup>\*,†</sup> and Jianzhuang Jiang<sup>\*,†</sup>

Department of Chemistry, Shandong University, Jinan 250100, China, Department of Chemistry, Jinan University, Jinan 250001, China, Institute of Chemistry, Chinese Academy of Science, Beijing 100080, China, and Department of Chemistry, Northwestern University, Evanston, Illinois 60208-3113

Received December 24, 2006. In Final Form: February 9, 2007

A novel perylene diimide (PDI) derivative with typical amphiphilic character, **2**, was designed and prepared. The spectroscopic studies on this compound in solution revealed the face-to-face dimeric configuration and effective  $\pi$ - $\pi$  interaction between the two perylene rings. This amphiphilic PDI derivative was fabricated into highly ordered films by Langmuir-Blodgett (LB) technique and fabricated into an organic field effect transistor (OFET), which shows carrier mobility around  $0.05 \text{ cm}^2 \text{ V}^{-1} \text{ s}^{-1}$  and current modulation of  $10^3$ . This OFET performance is much better than that of monomeric PDI **1** and can be attributed to the unique face-to-face structure of **2**, which promotes the interactions between neighboring PDI ring in LB film as indicated by the  $\pi$ -A isotherms and UV-vis absorption.

## Introduction

Organic semiconductors have been the focus of many current research interests because of the great potential applications of organic field effect transistor (OFET) in low cost memory, price tags, and driving circuits for large area and flexible display devices. Significant progress has been made in the past decade toward understanding OFETs and improving their performance. This has clearly been revealed by the high carrier mobility and current modulation of OFETs reached, which are comparable with those of amorphous hydrogenated silicon (a-Si:H) counterparts.<sup>1-9</sup>

In addition to the intrinsic molecular chemical-physical properties and electronic structures of organic compounds, the performance of OFETs has been found to be closely related with the packing model of organic molecules in the solid state.<sup>10-12</sup> Exploration of the relationship between the packing model of organic semiconductor molecules in the solid state and the device performance has thus been an important topic in this field. It has generally been accepted that maximizing  $\pi$ -orbital overlap between neighboring conjugated molecules is one good way to construct organic semiconductor thin films to reach high carrier

mobility.<sup>13-19</sup> Various methods have been developed to enhance face-to-face stacking of conjugated semiconductor molecules in solid state by introducing different functional groups which are able to drive the assembly process to the prerequisite stacking. For instance, substituents were incorporated to pentacene molecules to prevent C-H $\cdots$  $\pi$  forces and induce more effective  $\pi$ - $\pi$  interactions between pentacene molecules, thus leading to improved OFET properties.<sup>20-22</sup> Introduction of long alkoxy groups onto aromatic semiconductor molecules was also found to be helpful in improving the OFET properties as the liquid crystal property borrowed beneficial in promoting the  $\pi$ - $\pi$  stacking and form ordered structure.<sup>23,24</sup> Dimerization of oligo-thienylenevinylenes (nTVs) on the substrate was lately proven to also significantly promote the carrier mobility of corresponding OFETs.<sup>25,26</sup> With this in mind, it is reasonable to assume that constructing the monomeric aromatic semiconductor molecules into a dimeric double-decker structure will be a good strategy to enhance the OFET performance of corresponding materials.

\* To whom correspondence should be addressed. E-mail: xiyouli@sdu.edu.cn (X.L.) or jzjiang@sdu.edu.cn (J.J.).

<sup>†</sup> Shandong University.

<sup>‡</sup> Jinan University.

<sup>§</sup> Chinese Academy of Science.

<sup>||</sup> Northwestern University.

(1) Garnier, F. *Acc. Chem. Res.* **1999**, *32*, 209–215.

(2) Horowitz, G. *Adv. Mater.* **1998**, *10*, 365–377.

(3) O'Neil, M.; Kelly, S. M. *Adv. Mater.* **2003**, *15*, 1135–1146.

(4) Perepichka, I. F.; Perepichka, D. F.; Meng, H.; Wudl, F. *Adv. Mater.* **2005**, *17*, 2281–2305.

(5) Sun, Y.; Liu, Y.; Zhu, D. *J. Mater. Chem.* **2005**, *15*, 53–65.

(6) Gundlach, D. J.; Lin, Y. Y.; Jackson, T. N.; Nelson, S. F.; Schlom, D. G. *IEEE Electron Device Lett.* **1997**, *18*, 87–89.

(7) Lin, Y. Y.; Gundlach, D. J.; Nelson, S. F.; Jackson, T. N. *IEEE Electron Device Lett.* **1997**, *18*, 606–608.

(8) Afzali, A.; Dimitrakopoulos, C. D.; Breen, T. L. *J. Am. Chem. Soc.* **2002**, *124*, 8812–8813.

(9) Mas-Torrent, M.; Durkut, M.; Hadley, P.; Ribas, X.; Rovira, C. *J. Am. Chem. Soc.* **2004**, *126*, 984–985.

(10) Dimitrakopoulos, C. D.; Brown, A. R.; Pomp, A. *J. Appl. Phys.* **1996**, *80*, 2501–2508.

(11) Dimitrakopoulos, C. D.; Mascaro, D. J. *IBM J. Res. Dev.* **2001**, *45*, 11–27.

(12) Xiao, K.; Liu, Y. Q.; Yu, G.; Zhu, D. B. *Appl. Phys. A* **2003**, *77*, 367–370.

(13) Bendikov, M.; Wudl, F.; Perepichka, D. F. *Chem. Rev.* **2004**, *104*, 4891–4945.

(14) Facchetti, A.; Yoon, M.-H.; Stern, C. L.; Hutchison, G. R.; Ratner, M. A.; Marks, T. J. *J. Am. Chem. Soc.* **2004**, *126*, 13480–13501.

(15) Kwon, O.; Coropceanu, V.; Gruhn, N. E.; Durivage, J. C.; Laquindanum, J. G.; Katz, H. E.; Cornil, J.; Brédas, J. L. *J. Chem. Phys.* **2004**, *120*, 8186–8194.

(16) Hutchison, G. R.; Ratner, M. A.; Marks, T. J. *J. Am. Chem. Soc.* **2005**, *127*, 16866–16881.

(17) Halik, M.; Klauk, H.; Zschieschang, U.; Schmid, G.; Ponomarenko, S.; Kirchmeyer, S.; Weber, W. *Adv. Mater.* **2003**, *15*, 917–922.

(18) Facchetti, A.; Yoon, M.-H.; Stern, C. L.; Katz, H. E.; Marks, T. J. *Angew. Chem., Int. Ed.* **2003**, *42*, 3900–3903.

(19) Miao, Q.; Lefenfeld, M.; Nguyen, T.-Q.; Siegrist, T.; Kloc, C.; Nuckolls, C. *Adv. Mater.* **2005**, *17*, 407–412.

(20) Anthony, J. E.; Eaton, D. L.; Parkin, S. R. *Org. Lett.* **2002**, *4*, 15–18.

(21) Anthony, J. E.; Brooks, J. S.; Eaton, D. L.; Parkin, S. R. *J. Am. Chem. Soc.* **2001**, *123*, 9482–9483.

(22) Meng, H.; Bendikov, M.; Mitchell, G.; Holgeson, R.; Wudl, F.; Bao, Z.; Siegrist, T.; Kloc, C.; Chen, C.-H. *Adv. Mater.* **2003**, *15*, 1090–1093.

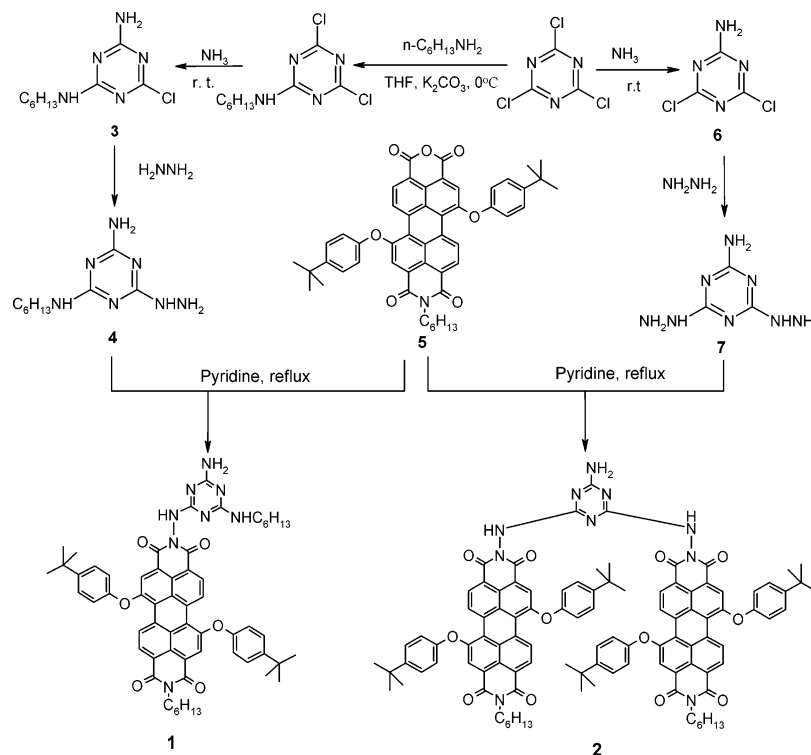
(23) Simpson, C. D.; Wu, J.; Watson, M. D.; Müllen, K. *J. Mater. Chem.* **2004**, *14*, 494–504.

(24) An, Z.; Yu, J.; Jones, S. C.; Barlow, S.; Yoo, S.; Domercq, B.; Prins, P.; Siebbeles, L. D. A.; Kippelen, B.; Marder, S. R. *Adv. Mater.* **2005**, *17*, 2580–2583.

(25) Videlet, C.; Ackermann, J.; Blanchard, P.; Raimundo, J. M.; Frère, P.; Allian, M.; Bettignies, R.; Levillain, E.; Roncali, J. *Adv. Mater.* **2003**, *15*, 306–310.

(26) Sokolov, A. N.; Friščić, T. L.; MacGillivray, R. *J. Am. Chem. Soc.* **2006**, *128*, 2086–2087.

Scheme 1. Synthesis of the PDI Monomer 1 and Dimer 2



Perylene tetracarboxyl diimides (PDIs), a category of organic dyes with excellent thermal and photostability, have recently been intensively studied as good n-type semiconductors due to the high electron affinity caused by the electron-withdrawing imide groups.<sup>27–29</sup> Different functional groups have been introduced at the imide nitrogen atoms of PDIs with the aim of modifying the packing in solid state and thus improving the OFETs performance.<sup>2,28,30–32</sup> Electron withdrawing groups, such as cyanide groups, introduced to the bay positions have been proved to improve the n-type semiconductivity significantly.<sup>33</sup> Solution processed films of PDIs have been fabricated into OFETs recently, and ambipolar transport properties for PDI were observed for the first time.<sup>34</sup>

In the present paper, we report the design and synthesis of a novel PDI compound with phenoxy groups at the bay positions and hydrophobic alkyl substituents at one of the two imide nitrogens of the PDI molecule. More interestingly, two of these PDI rings were linked by a hydrophilic triazine ring to form a PDI double-decker dimer with very good amphiphilic properties, Scheme 1. Good OFETs performance using Langmuir–Blodgett (LB) films of this compound as an active layer has been achieved with the carrier mobility as high as  $0.05 \text{ cm}^2 \text{ V}^{-1} \text{ s}^{-1}$  and current modulation of  $10^3$  which is much better than that of the LB films fabricated from the corresponding PDI monomer.

## Experimental Section

**General Remarks.** <sup>1</sup>H NMR spectra were recorded on a Bruker DPX 300 spectrometer (300 MHz) using SiMe<sub>4</sub> as reference. EI mass spectra were recorded on a Micromass Zabspec instrument. MALDI-TOF mass spectra were taken on a Bruker BIFLEX III ultrahigh-resolution Fourier transform ion cyclotron resonance (FT-ICR) mass spectrometer with  $\alpha$ -cyano-4-hydroxycinnamic acid as the matrix. Electronic absorption spectra were recorded on a Hitachi U-4100 spectrophotometer, whereas the fluorescence spectra and fluorescence lifetime were recorded on ISIS K2 system (U.S.A.). Elemental analyses were performed by the Institute of Chemistry, Chinese Academy of Sciences. Electrochemical measurements were carried out on a BAS CV-50W voltammetric analyzer with a glassy carbon disk working electrode (2.0 mm in diameter), a silver-wire counter electrode, and an Ag/Ag<sup>+</sup> reference electrode. The experiments were carried out under nitrogen at room temperature. Tetrabutylammonium perchlorate in freshly distilled CH<sub>2</sub>Cl<sub>2</sub> ( $0.1 \text{ mol dm}^{-3}$ ) was used as the electrolyte solution. Ferrocene was employed as the reference redox system according to IUPAC's recommendation.<sup>35</sup> Low angle X-ray diffraction (LAXRD) experiments were carried out on a Rigaku D/max- $\gamma$ B X-ray diffraction system.

**Thin Film Deposition and Characterization.** The monolayer was prepared by spreading a solutions of PDIs in CH<sub>2</sub>Cl<sub>2</sub> ( $0.11 \text{ mg/mL}$ ) onto the surface of ultrapure water (resistivity =  $18 \text{ M}\Omega \text{ cm}^{-1}$ , pH = 6.4) or barbituric acid aqueous solution. The monolayer properties were studied by measuring pressure–area isotherms at room temperature with a compression rate of  $20 \text{ cm}^2 \text{ min}^{-1}$  on a NIMA SYSTEM 622 LB trough (Great Britain). The literature method described by Höning et al.<sup>36</sup> was adopted to treat the substrates. All LB films for low-angle X-ray diffraction, UV–vis, and fluorescence spectroscopic measurements were deposited onto hydrophobic quartz plates by the vertical dipping method with a dipping speed of  $7 \text{ mm min}^{-1}$  while the surface pressure was kept at  $20 \text{ mN m}^{-1}$ . The time interval between two consecutive layer depositions was 15 min. The

(27) Würthner, F. *Angew. Chem., Int. Ed.* **2001**, *40*, 1037–1039.

(28) Kraft, A. *Chem. Phys. Chem.* **2001**, *2*, 163–165.

(29) Dimitrakopoulos, C. D.; Malenfant, P. R. L. *Adv. Mater.* **2002**, *14*, 99–117.

(30) Locklin, J.; Li, D.; Mannsfeld, S. C. B.; Borkent, E.-J.; Meng, H.; Advincula, R.; Bao, Z. *Chem. Mater.* **2005**, *17*, 3366–3374.

(31) Struijk, C. W.; Sieval, A. B.; Dakhorst, J. E. J.; Von Dijk, M.; Kimkes, P.; Koehorst, R. B. M.; Donker, H.; Schaafsma, T. J.; Picken, S. J.; Van de Craats, A. M.; Warman, J. M.; Zuilhof, H.; Sudhölter, E. J. R. *J. Am. Chem. Soc.* **2000**, *122*, 11057–11066.

(32) Chen, Z.; Debije, M. G.; Debaerdemaeker, T.; Osswald, P.; Würthner, F. *ChemPhysChem* **2004**, *5*, 137–140.

(33) Jones, B. A.; Ahrens, M. J.; Yoon, M.-H.; Facchetti, A.; Marks, T. J.; Wasielewski, M. R. *Angew. Chem., Int. Ed.* **2004**, *43*, 6363–6366.

(34) Singh, T. B.; Erten, S.; Günes, S.; Zafer, C.; Turkmen, G.; Kuban, B.; Teoman, Y.; Sariciftci, N. S.; Icli, S. *Org. Electron.* **2006**, *7*, 480–489.

(35) Gritzner, G. *Pure Appl. Chem.* **1990**, *62*, 1839.

(36) Höning, E. P.; Hengst, J. H. T.; Engels, D. D. *J. Colloid Interface Sci.* **1973**, *45*, 92–102.

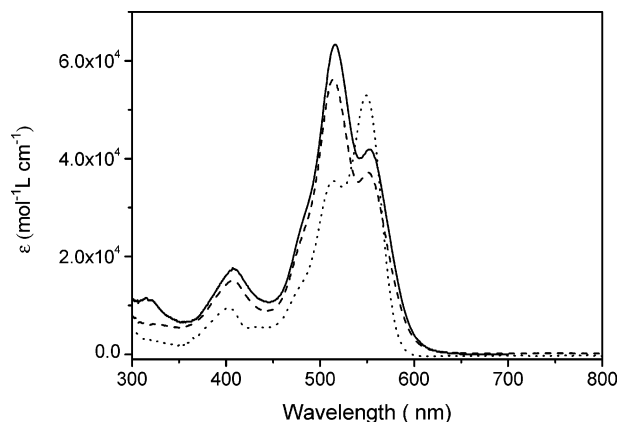


**Figure 1.** UV-vis spectra of **2** in chloroform (solid) and toluene (dash) with monomeric **1** in chloroform (dot) as reference (concentration of the solution:  $1 \times 10^{-5}$  mol L $^{-1}$ ).

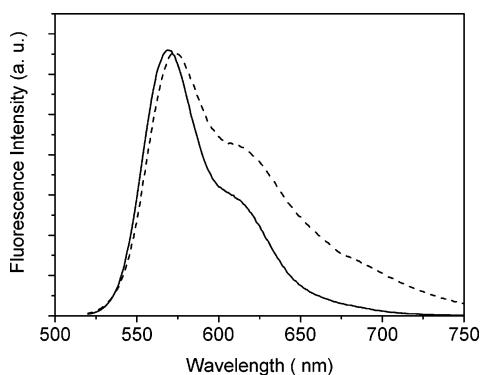


**Figure 2.** Normalized fluorescence spectra of monomer **1** (solid) and dimer **2** (dash) in toluene (excitation at 410 nm, concentration of the solution:  $5 \times 10^{-6}$  mol L $^{-1}$ ).

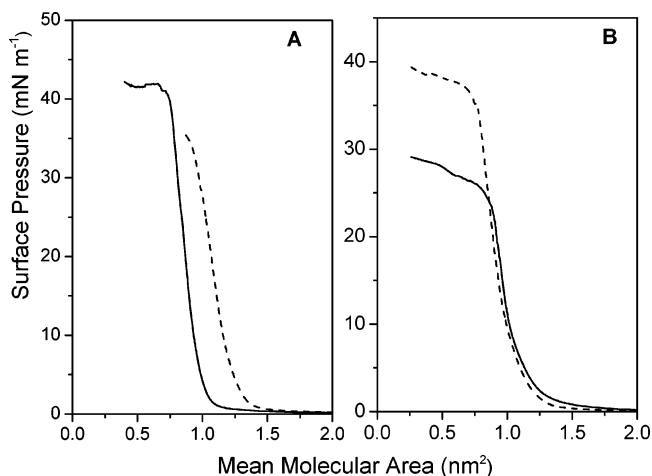


**Figure 3.**  $\pi$ -A isotherms of **1** (A) and **2** (B) on the surface of water (solid line) and barbituric acid solution (dash line).

transfer ratio was found to be unity for both monomeric **1** and dimeric **2** on different subphases.

**OFET Device Fabrication.**<sup>37</sup> A heavily doped silicon layer was used as the gate electrode. The oxide layer with a thickness of 400 nm covering the surface of the silicon gate electrode is the gate dielectric having a capacitance per unit area of 10 nF cm $^{-2}$ . After the LB film deposition onto the surface of this oxide layer, the source/drain electrodes were thermally evaporated onto the LB films by use of a shadow mask. The channel width ( $W$ ) and length ( $L$ ) of these source/drain electrodes are 28.6 and 0.24 mm respectively and

the ratio of width to length ( $W/L$ ) was then 119. The electric characteristics of these devices were measured in air at ambient temperature with a Hewlett-Packard (HP) 4140B parameter analyzer.

**Synthesis.** Column chromatography was carried out on silica gel (Merck, Kieselgel 60, 70–230 mesh) with the indicated eluents. All other reagents and solvents were used as received. 1-Amino-3-hexylamino-5-chloro-2,4,6-triazine (**3**),<sup>38</sup> 1-amino-3,5-dichloro-2,4,6-triazine (**6**),<sup>39</sup> and 1,7-di(*t*-butyl)phenoxy-perylene-3,4,9,10-tetracarboxy dianhydride (**8**)<sup>40</sup> were prepared following the literature methods.

**1-Amino-3-hexylamino-5-hydrazine-2,4,6-triazine (4).** 1-Amino-3-hexylamino-5-chloro-2,4,6-triazine (**3**) (2.3 g, 0.01 mol) was mixed with an excess of hydrazine in THF and reacted at room temperature overnight. The reaction mixture was diluted with water, and the solid formed was collected by filtration. After being washed with water thoroughly for several times, the solid was dried at ambient temperature to give product **4** (2.1 g, yield 94%). MS (EI): Calcd. for C<sub>10</sub>H<sub>19</sub>N<sub>5</sub>, 209.30; Found, 210.

**1,7-Di(*t*-butyl)phenoxy-perylene-9,10-(*N*-hexyl)-dicarboximide-3,4-dicarboxy anhydride (5).** The solution of 1,7-Di(*t*-butyl)phenoxy-perylene-3,4,9,10-tetracarboxy dianhydride (1.4 g, 2.0 mmol) in pyridine (100 mL) was purged with dry nitrogen for 15 min and then was heated to reflux. To this solution was slowly added hexylamine (200 mg, 2 mmol) in pyridine (10 mL) over the course of 30 min. The resulting mixture was refluxed continuously for another 30 min, and then, the volatiles were removed under reduced pressure. The residue was column chromatographed on silica gel with chloroform as the eluent. Repeated chromatography followed by recrystallization from a mixture of CHCl<sub>3</sub> and MeOH gave pure **5** (980 mg, yield 64%). <sup>1</sup>H NMR (CDCl<sub>3</sub>, 300 MHz):  $\delta$  9.64 (d,  $J$  = 8.4 Hz, 2H), 8.58–8.62 (d+d,  $J$  = 8.4 Hz, 2H), 8.35 (s+s, 2H), 7.52 (m, 4H), 7.14 (m, 4H), 4.15 (t,  $J$  = 7.2 Hz, 2H), 1.73 (br, 2H), 1.40 (s, 18H), 1.27–1.38 (br, 6H), 0.90 (br, 3H). MS (MALDI-TOF): Calcd. for C<sub>50</sub>H<sub>45</sub>NO<sub>7</sub>, 772; Found, 771. Elemental Anal. Calcd. for C<sub>50</sub>H<sub>45</sub>NO<sub>7</sub>: C, 77.80; H, 5.88; N, 1.91. Found: C, 77.12; H, 6.01; N, 2.01.

**Monomeric PDI (1).** The mixture of **4** (14 mg, 0.06 mmol) and **5** (55 mg, 0.07 mmol) in 15 mL of pyridine was heated to reflux under nitrogen and kept at this temperature overnight. After the solvent was evaporated under reduced pressure, the residue was purified by column chromatography on silica gel with a mixture of chloroform/methanol (96/4) as eluent. **1** was collected as red solid from the second red fraction (24 mg, yield 39.4%). <sup>1</sup>H NMR (CDCl<sub>3</sub>, 300 MHz):  $\delta$  9.54 (d,  $J$  = 8.3 Hz, 2H), 8.52 (d+d,  $J$  = 8.3 Hz, 2H), 8.30 (s+s, 2H), 7.48 (m, 4H), 7.08 (m, 4H), 5.05 (br, 2H), 4.15 (t,  $J$  = 7.0 Hz, 2H), 3.20 (br, 2H), 1.75 (br, 8H), 1.37 (s, 18H), 1.21–1.32 (br, 8H), 0.90 (br, 6H). MS (MALDI-TOF): Calcd for C<sub>59</sub>H<sub>62</sub>N<sub>8</sub>O<sub>6</sub>, 979.2; Found, 979.7. Elemental Anal. Calcd. for C<sub>59</sub>H<sub>62</sub>N<sub>8</sub>O<sub>6</sub>: C, 72.37; H, 6.38; N, 11.44. Found: C, 72.12; H, 6.41; N, 12.01.

**1-Amino-3,5-dihydrazine-2,4,6-triazine (7).** A mixture of 1-amino-3,5-dichloro-2,4,6-triazine (**6**) (0.5 g, 3.03 mmol) and hydrazine (4 mL) in methanol (20 mL) was stirred at room temperature for 10 h. A white solid (0.38 g, yield 80%) was collected by filtration. <sup>1</sup>H NMR (DMSO-*d*<sub>6</sub>, 300 Mz):  $\delta$  7.76 (br, 2H), 6.34 (br, 2H), 4.21 (br, 4H). MS (EI): Calcd. for C<sub>3</sub>H<sub>8</sub>N<sub>8</sub>, 156; Found, 156.

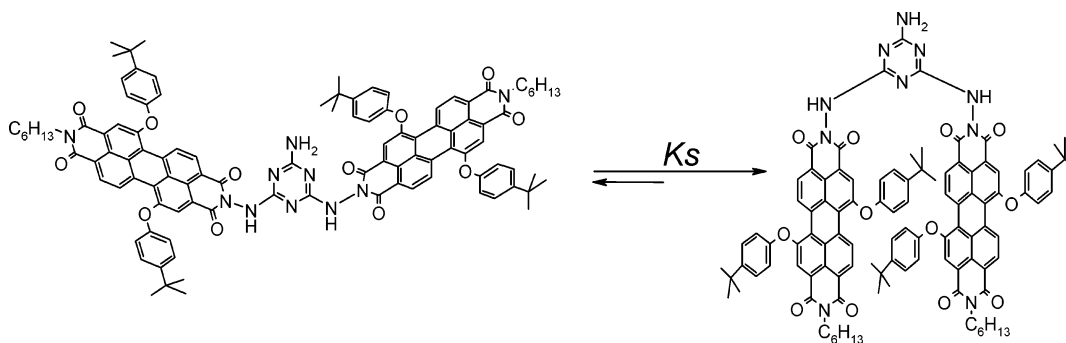
**PDI Dimer (2).** The mixture of **7** (10 mg, 0.066 mmol) and **5** (105 mg, 0.132 mmol) in pyridine (25 mL) was refluxed for 10 h under nitrogen. After removing the solvents under reduced pressure, the residue was column chromatographed on silica gel with CHCl<sub>3</sub>/ethyl acetate (1:1) as eluent. Repeated chromatography followed by recrystallization from a mixture of CHCl<sub>3</sub> and MeOH gave pure **2** as a purple solid (35 mg, yield 32.8%). <sup>1</sup>H NMR (CDCl<sub>3</sub>, 300 MHz):  $\delta$  9.12 (d,  $J$  = 8.0 Hz, 4H), 8.08 (d+d,  $J$  = 8.0 Hz, 4H), 7.95 (s+s, 4H), 7.84 (br, 2H), 7.36 (m, 8H), 6.96 (m, 8H), 6.18 (br, 2H), 4.07 (br, 4H), 1.69 (br, 4H), 1.25–1.34 (br, 48H), 0.88 (br, 6H). MS (MALDI-TOF): Calcd for C<sub>103</sub>H<sub>94</sub>N<sub>10</sub>O<sub>12</sub>, 1663.9; Found, 1663.9.

(38) Bielejewska, A. G.; Marjo, C. E.; Prins, L. J.; Timmerman, P.; Jong, F.; Reinhoudt, D. N. *J. Am. Chem. Soc.* **2001**, *123*, 7518–7533.

(39) Würthner, F.; Thalacker, C.; Sautter, A. *Adv. Mater.* **1999**, *11*, 754–758.

(40) van der Boom, T.; Hayes, R. T.; Zhao, Y.; Bushard, P. J.; Weiss, E. A.; Wasielewski, M. R. *J. Am. Chem. Soc.* **2002**, *124*, 9582–9590.

(37) Su, W.; Jiang, J.; Xiao, K.; Chen, Y.; Zhao, Q.; Yu, G.; Liu, Y. *Langmuir* **2005**, *21*, 6527–6531.

Scheme 2. Equilibrium between Noncofacial and Face-to-Face Conformations for **2** in Solution

Elemental Anal. Calcd. for  $C_{103}H_{94}N_{10}O_{12}$ : C, 74.35; H, 5.69; N, 8.42. Found: C, 74.32; H, 5.80; N, 8.51.

## Results and Discussion

**Molecular Design and Synthesis.** This dimeric PDI **2** was designed with the idea of increasing the face-to-face interactions of neighboring PDIs in mind since many examples have revealed that large face-to-face interaction between neighboring molecules are beneficial to the performance of OFETs.<sup>20–26</sup> The linkage, triazine ring, used to connect two monomeric PDI units in compound **2**, is well-known for its hydrogen bonding with barbituric acid and forming face-to-face conformation for the connected two chromophores<sup>41–46</sup> and therefore provides possibility for ordering the molecules of compound **2** in solid film through hydrogen bonding.<sup>47–52</sup> The target compound was prepared following the procedure shown in Scheme 1. For the purpose of comparative studies, the monomeric PDI **1** was also prepared following a similar method. Both the monomeric **1** and dimeric **2** show very good solubility in organic solvents, which renders it possible to fabricate this compound into OFETs through solvent-based procedure especially by LB technique due to the typical amphiphilic nature.

**Configuration in Solution.** Figure 1 compares the electronic absorption spectra of monomeric **1** and dimeric **2** in solution. As shown in the graph, the main absorption band for dimeric **2** appears at about 515 nm, which is blue-shifted compared with that of monomeric **1**, indicating the strong face-to-face  $\pi$ – $\pi$  interaction in the double-decker molecules.<sup>53,54</sup> It is worth noting that the excimer's emission might result from the intermolecular aggregation of PDI dimers rather than the intramolecular  $\pi$ – $\pi$  stacking in compound **2**. However, the fact that no change was

observed in the electronic absorption spectra of dimeric **2** in toluene in the concentration range of  $1 \times 10^{-4}$  to  $1 \times 10^{-6}$  mol  $L^{-1}$  indicates that the blue shift in the main absorption band of dimeric **2** compared with monomeric **1** is indeed due to the intramolecular  $\pi$ – $\pi$  stacking.

As displayed in Figure 2, fluorescence spectrum of dimeric **2** in toluene shows a new shoulder around 685 nm with a total fluorescence quantum yield of 12% compared with that of monomeric PDI **1**. We ascribed the big tail to the excimer's emission which characterized with red-shifted emission band, low fluorescence quantum yield, and longer fluorescence lifetime.<sup>54</sup> This explanation has also been supported by the fluorescence lifetime measurement of the dimer in toluene which presents two lifetimes, 4.5 and 20.5 ns. The short one is attributed to the monomer's emission, whereas the longer one can be attributed to the excimer's emission as observed for a rigid face-to-face PDI dimer.<sup>54</sup> The strong emission peak at ca. 580 nm was ascribed to the monomeric PDI's emission, which suggested the equilibrium between the face-to-face and noncofacial conformation of **2** in solution, Scheme 2. This appears to contradict the results of the absorption spectra, which shows exclusively the absorption of face-to-face dimer but merely has to do with the detection limits of the two methods. Monomeric PDI has a fluorescence quantum yield near 100% and is a much higher than the excimer. A few percent of monomeric PDI will easily be detected by fluorescence, but not by absorption, where the extinction coefficients of the various states are on the same order of magnitude.<sup>53</sup> With 1,7-di(4'-*t*-butyl)phenoxy-perylene-3,4,9,10-(*N,N'*-dioctyl)dicarboxyimide as a standard, the concentration of the noncofacial molecules in the solution was determined by fluorescence spectrum and the equilibrium constant ( $K_s$ ) was calculated as around 50.

The face-to-face conformation of this compound was also confirmed by its <sup>1</sup>H NMR spectroscopic result. As shown in the Experimental Section, protons of perylene ring in the dimeric **2** resonate at  $\delta$  9.12 (protons at positions 6 and 12), 8.08 (protons at positions 5 and 11), and 7.95 (protons at positions 2 and 8), respectively. However, the corresponding protons in monomeric PDI **1** show signals at  $\delta$  9.54, 8.52, and 8.30, respectively. This high field shift may be due to the shielding effect of the ring current from the neighboring perylene ring in the dimeric **2** with a face-to-face conformation.

Additionally, the minimized structure of **2** obtained from AM1 calculation indicates that the face-to-face configuration of compound **2** is very stable with a center-to-center distance of 0.5 nm.<sup>55</sup> This theoretical short distance is consistent with the possible strong  $\pi$ – $\pi$  interactions between two PDI rings.

(41) Whitesides, G. M.; Simanek, E. E.; Mathias, J. P.; Seto, C. T.; Chin, D. N.; Mammen, M.; Gordon, D. M. *Acc. Chem. Res.* **1995**, *28*, 37–44.

(42) Lehn, J.-M. *Supramolecular Chemistry*; VCH: Weinheim, Germany, 1995; pp 161–179.

(43) Seto, C. T.; Whitesides, G. M. *J. Am. Chem. Soc.* **1993**, *115*, 905–906.

(44) Whitesides, G. M.; Mathias, J. P.; Simanek, E. E. *J. Am. Chem. Soc.* **1994**, *116*, 4326–4330.

(45) Mammen, M.; Simanek, E. E.; Whitesides, G. M. *J. Am. Chem. Soc.* **1996**, *118*, 12614–12623.

(46) Ishi-i, T.; Crego-Calama, M.; Timmerman, P.; Reinhoudt, D. N.; Shinkai, S. *J. Am. Chem. Soc.* **2002**, *124*, 14631–14641.

(47) Ni, Y.; Puthenkavilakom, R. R.; Huo, Q. *Langmuir* **2004**, *20*, 2765–2771.

(48) Weck, M.; Fink, R.; Ringsdorf, H. *Langmuir* **1997**, *13*, 3515–3522.

(49) Koyano, H.; Bissel, P.; Yoshihara, K.; Ariga, K.; Kunitake, T. *Chem. Eur. J.* **1997**, *3*, 1077–1082.

(50) Huo, Q.; Russell, K. C.; Leblanc, R. M. *Langmuir* **1998**, *14*, 2174–2186.

(51) Huo, Q.; Dziri, L.; Desbat, B.; Russell, K. C.; Leblanc, R. M. *J. Phys. Chem. B* **1999**, *103*, 2929–2934.

(52) Hasegawa, T.; Hatada, Y.; Nishijo, J.; Umemura, J.; Huo, Q.; Leblanc, R. M. *J. Phys. Chem. B* **1999**, *103*, 7505–7513.

(53) Kasha, M.; Rawls, H. R.; El-Bayoumi, M. A. *Pure Appl. Chem.* **1965**, *11*, 371–392.

(54) Ahren, M. J.; Sinks, L. E.; Rybtchinski, B.; Liu, W.; Jones, B. A.; Giarmo, J. M.; Gusev, A. V.; Goshe, A.; Tiede, D. M.; Wasielewski, M. R. *J. Am. Chem. Soc.* **2004**, *126*, 8284–8294.

(55) AM1 calculations were performed using *HyperChem*; Hypercube, Inc.: Gainesville, FL.

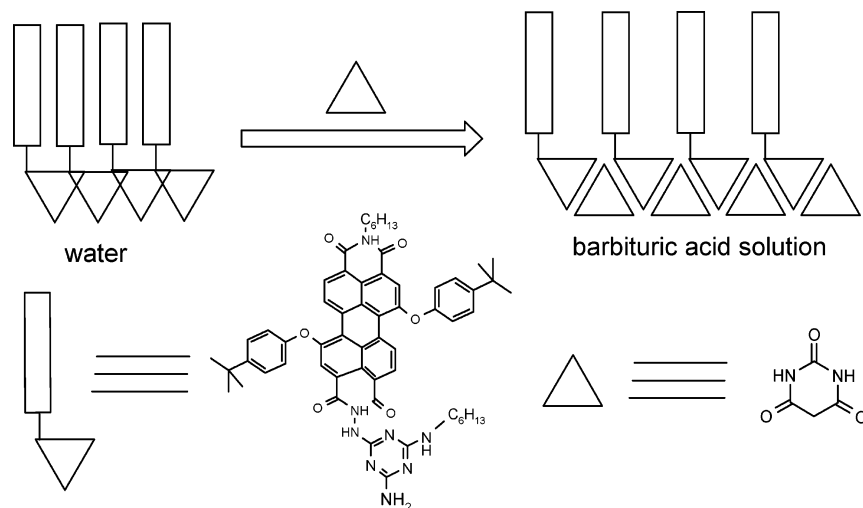


**Figure 4.** Schematic arrangement of compound **1** on the surface of water and barbituric acid solution.

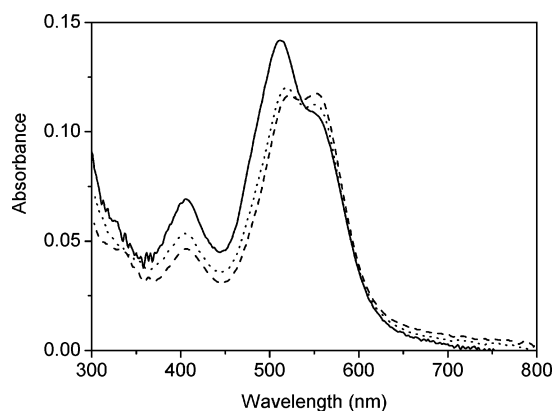


**Figure 5.** Electron absorption spectra of the 15 layer LB films of monomeric **1** deposited from water surface (dash) or from barbituric acid solution (dot) and 17 layer LB films of dimeric **2** from water surface (solid).

**Film Fabrication and Characterization. Monolayers.** Langmuir–Blodgett (LB) technique allows fine control of both the structure and the thickness of the film at molecular level and has been employed in building films for molecular electronics for a long time.<sup>56,57</sup> Both the monomeric **1** and dimeric **2** are typical amphiphilic compounds which can form stable monolayer on water surface. The  $\pi$ -*A* isotherm of compound **1** on pure water subphase gives a limiting molecular area of 0.94 nm<sup>2</sup>/molecule, Figure 3, which is close to that of the projection for a perpendicular standing molecule of compound **1** estimated from the minimized structure, 0.88 nm<sup>2</sup>/molecule,<sup>55</sup> indicating that molecules of **1** adopt a perpendicular edge-on configuration with triazine ring staying close to the water surface and the perylene rings obliged toward the air phase. On the surface of barbituric acid, the  $\pi$ -*A* isotherm of compound **1** is very similar to that on water surface except the increase of limiting molecular area to 1.20 nm<sup>2</sup>. We ascribed this to the formation of very stable hydrogen-bonding network between triazine ring and barbituric acid with expanding distance between the neighboring molecules, Figure 4.<sup>47,50</sup>

As also shown in Figure 3, compound **2** shows same  $\pi$ -*A* isotherm characteristics on the surface of both water and barbituric acid solution with almost the identical limiting molecular area of 1.08 nm<sup>2</sup>. This value is close to that of the projection for a perpendicular standing molecule of compound **2** estimated from

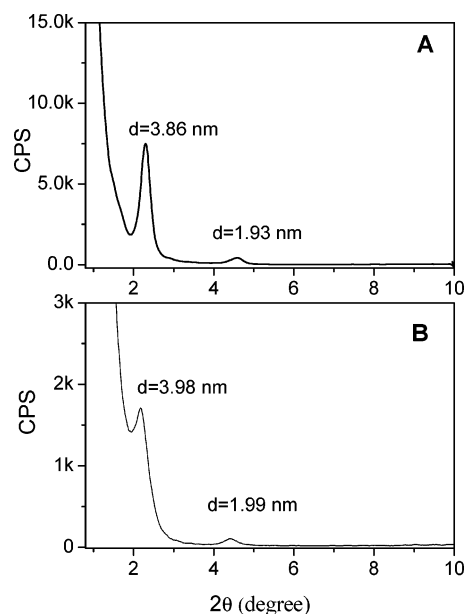


**Figure 6.** Low angle X-ray diffraction patterns for the LB films of **2** deposited from the surface of water (A) and barbituric acid solution (B).

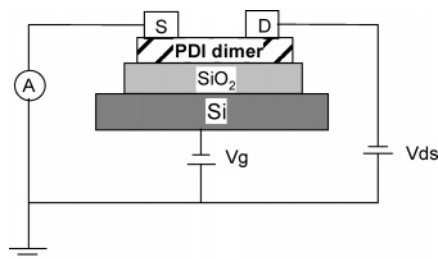


**Figure 7.** Schematic structure of the LB films based OFET device.

the minimized structure, 1.10 nm<sup>2</sup>/molecule, suggesting a perpendicular orientation for the molecules of compound **2** on the surface of water and barbituric acid solution and indicating such a fact that the barbituric acid in subphase increases the stability of the monolayers but add no effect on the orientation of the molecules of **2**. It is also worth noting that the limiting molecular area of **1** on the surface of water or barbituric acid solution is bigger than half of that for compound **2**, indicating a big distance and weak interaction between neighboring PDI units in the films of compound **1**.

(56) Ulman, A. *An Introduction to Ultrathin Organic Films: from Langmuir-Blodgett to Self-assembly*; Academic Press: San Diego, CA, 1991.

(57) Petty, M. C. *Thin Solid Films* **1992**, 210–211, 417–426.

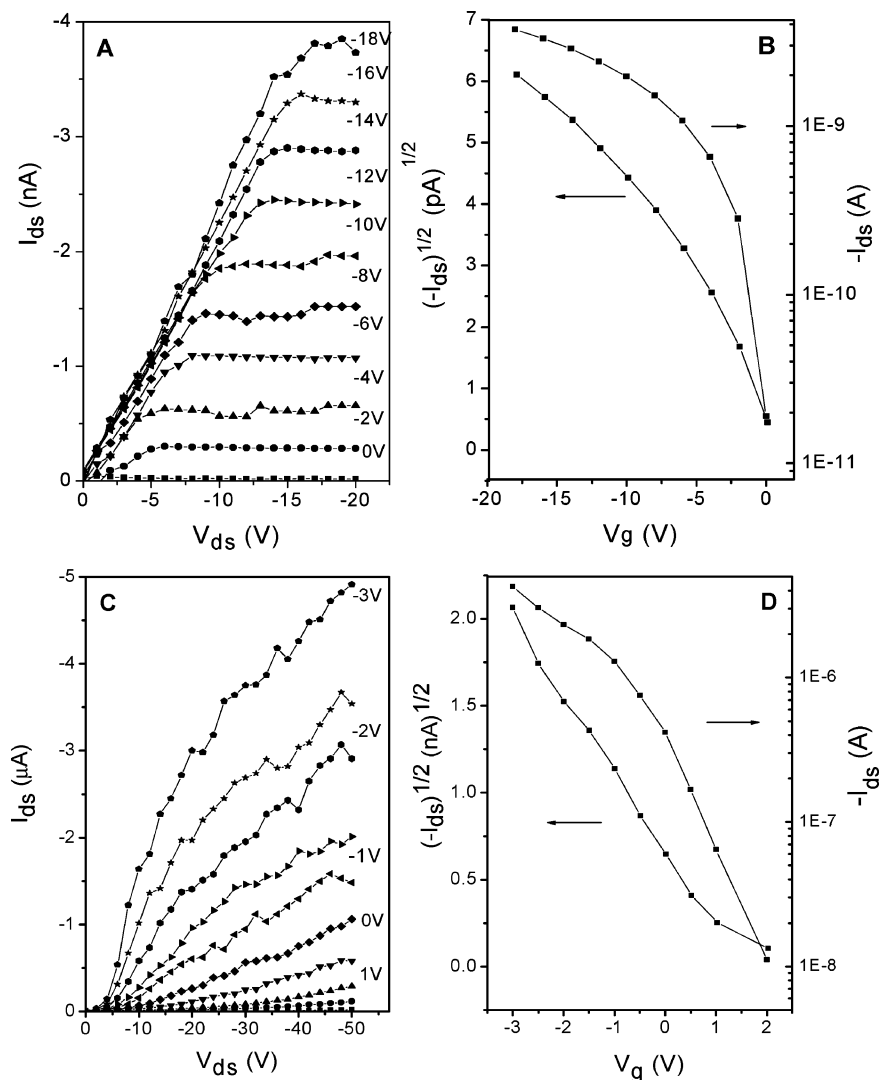


**Figure 8.** Current–voltage characteristics of LB-films of compound **1** (A) and **2** (C) deposited from the surface of water. Transfer characteristics of the device measured at a fixed source-drain voltage for **1** (B,  $V_{ds} = -20$  V) and **2** (D,  $V_{ds} = -40$  V).

**Multilayer LB Films.** Multilayer LB films of compounds **1** and **2** can be fabricated by vertical dipping method from the surface of water or barbituric acid solution. Because of the good amphiphilic properties of both compounds **1** and **2**, the transfer ratio during the film deposition for both of them is close to unity, indicating a very good layered structure for the LB films. The absorption spectra of dimeric **2** in LB films, Figure 5, show no significant shift in the main absorption band in comparison with that in solution, indicating the fact that the face-to-face dimeric structure is well preserved in the LB films. As also shown in Figure 5, the main absorption band of monomeric **1** in LB film blue shifts to 520 nm, suggesting the strong face-to-face  $\pi$ – $\pi$  interaction between neighboring molecules in the LB film. However, the shoulder at 550 nm due to the monomer species is obviously stronger than that of dimeric **2**, revealing the weak and incomplete  $\pi$ – $\pi$  interaction between neighboring molecules in the LB film of **1**.

The LB films of compounds **2** deposited from the surface of water or barbituric acid solution give clear diffraction peaks in their low angle X-ray diffraction (LAXRD) patterns, Figure 6, indicating very good layered structure. The  $d$  spaces calculated according to the Bragg equation are close to 4 nm and corresponding to the thickness of a double layer LB film (Y type). Comparison between these experimental results and the dimension of the molecules leads to such a conclusion that the

molecules are packing with the molecular plane perpendicular to the surface of the substrate in these LB films. This corresponds well with the result of monolayer studies that no rearrangement happened during the film transfer. It is worth noting that the  $d$  space of the LB film deposited from barbituric acid solution is a little bit bigger than that of the LB film deposited from water surface. This might be ascribed to the insertion of one layer of barbituric acid between each bilayer of PDI film via hydrogen bonding, which increases the interlayer thickness for the film deposited from barbituric acid solution. The LB films of monomeric **1** deposited from the surface of water and barbituric acid solution give similar X-ray diffraction patterns and  $d$  spaces with that of **2**, indicating similar layered structure and similar orientations of molecules in solid film.

**OFET Studies.** The OFET devices were fabricated with top contact configuration on a layer of  $\text{SiO}_2$  dielectrics (400 nm). Gold electrodes were applied after LB film deposition (21 layers) by using shadow mask, Figure 7. The devices were dried in vacuum at room temperature for several days before electronic testing.

The devices constructed from both the monomeric compound **1** and dimeric species **2** show typical  $p$ -channel characteristics as exhibited in Figure 8. We calculated the carrier mobility ( $\mu$ ) by using the saturation region transistor equation,  $I_{ds} = (W/2L)\mu C_0(V_g - V_t)^2$  and linear region transistor equation  $I_{ds} =$

$(W/L)\mu C_0(V_g - V_t)V_{ds}$ , where  $I_{ds}$  is the source-drain current,  $V_g$  the gate voltage,  $C_0$  the capacitance per unit area of the dielectric layer, and  $V_t$  the threshold voltage.<sup>58</sup> The LB film of monomeric **1** deposited from the surface of water gives a carrier mobility of  $9.1 \times 10^{-6} \text{ cm}^2 \text{ V}^{-1} \text{ s}^{-1}$ , whereas the one deposited from the surface of barbituric acid solution was failed to record any field effect. The LB film of dimeric compound **2** was revealed to show good OFET performance with carrier mobilities around 0.05 and  $0.06 \text{ cm}^2 \text{ V}^{-1} \text{ s}^{-1}$ , respectively, for the film deposited from pure water surface and from barbituric acid solution surface. The current modulations for both of them are  $10^3$ .

For monomeric **1**, the difference on the OFET performance between the LB films deposited from water and barbituric acid solution can be attributed to the different film structure as revealed by the  $\pi$ -A isotherms and UV-vis absorption spectra. The enlarged distance between two neighboring PDI molecules by the hydrogen-bonding network in the LB film deposited from the surface of barbituric acid solution hindered the moving of carriers between PDIs, Figure 4. The significantly improved OFET performance of the LB films of compound **2** over that of **1** can be rationalized by the strong interactions between PDI rings because of its unique dimeric molecular structure. The effective and intense  $\pi$ - $\pi$  interaction exists among the PDI rings in the dimeric molecules of **2**, facilitates the moving of holes between the molecules and results in good performance of corresponding OFETs fabricated. No obvious difference on the OFET performance between the LB films of dimeric **2** deposited from water and barbituric acid solution was observed. This is reasonable because the film structure was not affected by the hydrogen-bonding network as indicated by the  $\pi$ -A isotherms, UV-vis absorption spectra and LAXRD experiments.

As mentioned in the introduction section, PDIs are n-type organic semiconductors in all of the literature. However, our results suggest that both monomeric **1** and dimeric **2** show p-type characteristics. This might be ascribed to the electron donating

nature of the phenoxy groups at bay positions which decrease the redox potential and increase the HOMO energy level significantly. The electrochemical studies revealed that monomer **1** and dimer **2** give identical electrochemical characteristics with the first oxidation potential around 1.44 V (vs SCE). This is much smaller than that of the PDIs without substitution (1.6 V vs SCE). The smaller first redox potentials render **1** and **2** to produce holes with easy upon the negative gate bias and thus show p-type semiconductivity.<sup>59-62</sup>

### Conclusion

Two PDI rings were connected by a triazine ring form a PDI dimer with very stable face-to-face configuration in solution. This stable face-to-face configuration was kept and enforced in LB films. The unique face-to-face dimeric molecular structure of **2** together with high molecular ordering in the LB films ensures the strong inter- and intramolecular interaction in the LB film and good OFET performance. This result revealed that pre-organizing the organic molecules into a stacked structure in solution by covalent bond before the film fabrication might be an efficient way to improve its OFET performance.

**Acknowledgment.** The financial supports from NSFC (Grant No. 20571049, 20325105, 20431010, 20601017, and 50673051), Key lab of photochemistry of CAS, and Jinan University are acknowledged.

**Supporting Information Available:** The low angle XRD patterns for the LB film of monomeric **1**; the electronic absorption spectra of dimeric **2** in toluene at different concentrations; the data analysis of the fluorescence lifetime measurement by the phase modulation method. This material is available free of charge via internet at <http://pubs.acs.org>.

LA063729F

(59) Katz, H. E.; Bao, Z. N.; Gilat, S. L. *Acc. Chem. Res.* **2001**, *34*, 359-369.

(60) Facchetti, A.; Deng, Y.; Wang, A.; Koide, Y.; Siringhaus, H.; Marks, T. J.; Friend, R. H. *Angew. Chem., Int. Ed.* **2000**, *39*, 4547-4551.

(61) Facchetti, A.; Mushrush, M.; Katz, H. E.; Marks, T. J. *Adv. Mater.* **2003**, *15*, 33-38.

(62) Bao, Z. N.; Lovinger, A. J.; Dodabalapur, A. *Adv. Mater.* **1997**, *9*, 42-44.

(58) Sze, S. M. *Physics of Semiconductor Devices*; John Wiley & Sons: New York, 1981.